Self-Association Behavior of Hydrophobically Modified Poly(aspartic acid) in Water Studied by Fluorescence and Dynamic Light Scattering Techniques

Madoka Suwa, Akihito Hashidzume, and Yotaro Morishima*

Department of Macromolecular Science, Graduate School of Science, Osaka University, Toyonaka, Osaka 560-0043, Japan

Takeshi Nakato and Masayuki Tomida

Tsukuba Research Center, Mitsubishi Chemical Corporation, 8-3-1, Chuo, Ami, Inashiki, Ibaraki 300-0332, Japan

Received May 16, 2000; Revised Manuscript Received August 8, 2000

ABSTRACT: Poly(succinimide) (PSI), derived from L-aspartic acid by polycondensation, is a reactive precursor for synthesis of various derivatives of poly(aspartic acid) (PASP), a commercially interesting polyelectrolyte because of its biodegradable properties. Hydrophobically modified PASP was synthesized by reacting PSI with dodecylamine, followed by hydrolysis. The self-association behavior of PASP having pendant dodecyl groups (DDA-PASP) in water was characterized by fluorescence and quasielastic light scattering (QELS) techniques as a function of the mole percent content of dodecyl groups in the polymer (f_{Dod}). For fluorescence studies, the polymers were labeled singly with pyrene (Py-DDA-PASP) or doubly with naphthalene and pyrene (Np-Py-DDA-PASP). The vibrational fine structure of pyrene fluorescence spectra and the pyrene fluorescence lifetime for an aqueous solution of Py-DDA-PASP at pH = 9 indicated that associations of polymer-bound dodecyl groups started to occur at a low f_{Dod} (near 3 mol %), and a significant fraction of pyrene labels were incorporated in hydrophobic microdomains formed. Intrapolymer nonradiative energy transfer from naphthalene to pyrene in Np-Py-DDA-PASP indicated that a significant contraction of the conformational dimension occurred in the region $20 < f_{Dod} < 50$ mol % at pH = 9, this f_{Dod} region shifting to 10−30 mol % upon decrease in pH to 4 or upon addition of 0.05 M NaCl at pH = 9. QELS results at pH = 9 in the presence of 0.05 M NaCl indicated that DDA-PASP with $f_{Dod} \leq 31$ mol % forms two kinds of aggregates with well-defined hydrodynamic radii (R_h), R_h ranging 3−4 nm for one type of the aggregates and 60−90 nm for the other, and they are coexisting together. The fraction of the larger aggregates increases with polymer concentration. In contrast, DDA-PASP with $f_{Dod} = 48$ mol % forms only small aggregates with R_h on the order of 4 nm independent of the polymer concentration studied (0.25−1.0 g/dL). The mean aggregation number of dodecyl groups in this small aggregate was determined to be ca. 68 using a time-resolved fluorescence method. Since this aggregation number agrees well with the number of dodecyl groups per polymer chain (ca. 64) calculated from the degree of polymerization along with f_{Dod}, this small aggregate is suggested to be a unimolecular micelle. Accordingly, all the small aggregates with $R_h = 3-4$ nm found for the polymers with $f_{Dod} \leq 31$ mol % are also likely to be unimolecular micelles. Consequently, DDA-PASP exhibits a strong preference for intrapolymer hydrophobe self-associations to form a unimolecular micelle if the hydrophobe content is as high as 48 mol %.

Introduction

Polycondensation of L-aspartic acid (ASP) in the presence of a catalytic amount of *o*-phosphoric acid in an appropriate solvent (e.g., mesitylene) yields poly(succinimide) (PSI) which constitutes a succinimide (SI) moiety as the repeating unit.[1] Molecular weights of PSI are normally on the order of 10^4. Since this polymer is susceptible to ring-opening reactions with various nucleophiles, PSI is a useful precursor for syntheses of various types of ASP-based polymers. Upon hydrolysis of PSI in aqueous NaOH, poly(aspartic acid) (PASP) is obtained.[2] This PASP consists of ASP repeating units in the α- and *β*-form with a 28/72 ratio (Scheme 1), different from the polypeptide derived from ASP by ordinary peptide synthesis.[2] PASP is a commercially interesting polyelectrolyte because of its biodegradability and is expected to find an application as a sustainable water-absorbent material that may be used for diapers and hygienic goods.[3]

Using an alkylamine as a nucleophile to react with PSI, a polymer consisting of an alkyl group as its side chain can be obtained in a quantitative yield. As reported in an earlier paper, upon treating PSI with dodecylamine (DDA) in *N*,*N*-dimethylformamide (DMF), followed by hydrolysis, a DDA-modified PASP (DDA-PASP) (Chart 1) is obtained.[4] The degree of the hydrophobic modification of PASP, i.e., the mole percent content of dodecyl groups in the polymer (f_{Dod}), is primarily determined by the molar ratio of DDA to the SI unit of PSI in the reaction mixture. It has been confirmed that DDA-PASP is a biodegradable water-

Scheme 1. Structures of ASP Units in PASP Formed by Hydrolysis of PSI

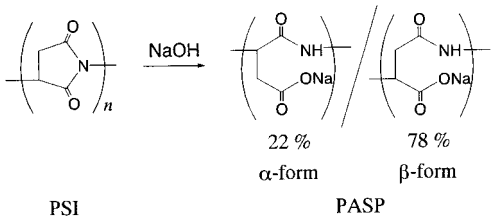

10.1021/ma0008342 CCC: $19.00
Published on Web 09/28/2000

Chart 1. Hydrophobically Modified PASP with and without Fluorescence Labels

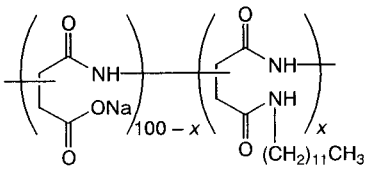

DDA-PASP

x = 0, 3, 14, 22, 31, and 48 mol %

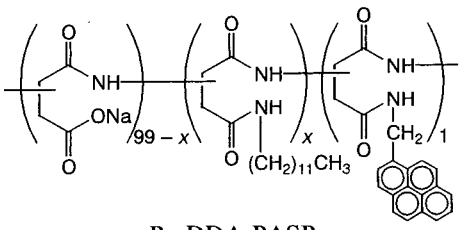

Py-DDA-PASP

x = 0, 4, 14, 22, 32, and 47 mol %

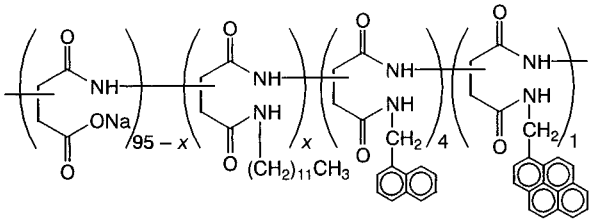

Np-Py-DDA-PASP

x = 0, 5, 12, 21, 31, and 43 mol %

soluble amphiphilic polyelectrolyte up to f_{Dod} = 46 mol %.[4]

Over the past decades, the self-association behavior of hydrophobically modified water-soluble polymers in aqueous media has received considerable interest from both scientific and practical perspectives.[5] Hydrophobically modified polyelectrolytes are among the polymers that have been extensively studied in the past decades. The self-association of polymer hydrophobes may occur either within a single polymer chain or between different polymer chains. Interpolymer hydrophobe associations may lead to the formation of network structures, whereas intrapolymer associations may lead to the formation of single macromolecular micelles (unimolecular micelles). A characteristic of hydrophobic self-associations in hydrophobically modified polyelectrolytes is that hydrophobic associations compete with electrostatic repulsions, showing a marked tendency of intra- vs interpolymer hydrophobe associations strongly depending on macromolecular architectures. For example, random copolymers of sodium 2-(acrylamido)-2-methylpropanesulfonate (AMPS) and *N*-dodecylmethacrylamide (DodMAm) undergo predominant intrapolymer hydrophobic self-association in aqueous solutions even at high polymer concentrations.[6−10] In contrast, random copolymers of AMPS and dodecyl methacrylate (DMA)[11] show a strong tendency for interpolymer association. This comparison indicates that associative properties of hydrophobes linked to a polyelectrolyte via amide and ester spacer bonds are remarkably different. Amide-linked hydrophobes exhibit a strong tendency for intrapolymer association whereas ester-linked hydrophobes are prone to undergo interpolymer association. Besides spacer bonding, structural factors that affect the preference of intra- or interpolymer hydrophobe association include the number of hydrophobes per polymer chain and their distribution on a polymer chain. Blocky hydrophobe distributions exhibit a tendency for interpolymer association whereas random distributions show a tendency for intrapolymer association.[12] There is a trend that interpolymer associations occur favorably when the hydrophobe content is low whereas intrapolymer associations become more favorable when the hydrophobe content is increased.[7−9,13]

DDA-PASP is an amphiphilic polyelectrolyte in which dodecyl moieties are linked to the polymer backbone via an amide spacer, and their distribution in the polymer chain should be virtually random. From these structural features, DDA-PASP is expected to exhibit a preference for intrapolymer hydrophobe association.

A purpose of this work is to elucidate the association behavior of DDA-PASP in aqueous solutions as a function of f_{Dod}. For characterization, various fluorescence and quasielastic light scattering (QELS) techniques were employed. For fluorescence studies, the polymers labeled singly with pyrene (Py-DDA-PASP) or doubly with naphthalene and pyrene (Np-Py-DDA-PASP) were employed (Chart 1). As mentioned above, hydrophobe association occurs competing with electrostatic repulsions among charged groups, and hence the hydrophobe/charge ratio in a polymer is a critical factor for the self-association. Therefore, we focused on effects of pH and ionic strength on the self-association behavior of DDA-PASP.

Experimental Section

Materials. DDA-PASP, Py-DDA-PASP, and Np-Py-DDA-PASP (Chart 1) were synthesized at the Tsukuba Research Center of Mitsubishi Chemical Corporation. PSI, a precursor for PASP, was synthesized by polycondensation of L-aspartic acid in the presence of a catalytic amount of *o*-phosphoric acid.[1,2] PSI was reacted with a predetermined amount of dodecylamine in dry DMF at 100 °C, followed by hydrolysis with aqueous NaOH under ice cooling to obtain DDA-PASP. The details of the synthesis of DDA-PASP have been reported elsewhere.[4] The pyrene-labeled polymers were synthesized by reacting PSI with a mixture of predetermined amounts of dodecylamine and 1-pyrenylmethylamine, followed by hydrolysis. The doubly labeled polymers were synthesized employing a mixture of dodecylamine, 1-pyrenylmethylamine, and 1-naphthylmethylamine of a predetermined molar ratio for reacting with PSI. The contents of the dodecyl moieties in the polymers were determined by ^{1}H NMR using a resonance band peaking at 1.1 ppm due to methyl protons in the dodecyl group and that at 1.5, 1.7, or 3.4 ppm due to methylene protons in the dodecyl group along with a resonance band peaking at 2.8−3.1 ppm due to methylene protons in PASP and that at 4.7 or 4.9 ppm associated with methine protons in PASP. The contents of pyrene and naphthalene labels in the singly and doubly labeled polymers were determined by ^{1}H NMR and UV absorption spectroscopy.

Pyrene was purchased from Nacalai Tesque and purified by recrystallization from ethanol. 1,6-Diphenyl-1,3,5-hexatriene (DPH) was purchased from Nacalai Tesque and used as received. Analytical grade sodium chloride, sodium hydroxide, and hydrochloric acid were used without further purification. Water used for the preparation of polymer solutions was purified with a Millipore Milli-Q system.

Measurements. a. Gel Permeation Chromatography (GPC). Measurements were performed at 80 °C with a GPC system composed of JASCO 880-PU pumps, a JASCO 860-CO column oven, PLgel MIXED-C columns (Polymer Laboratory, pore size: 5 μm), a JASCO 830-RI detector, and a TOSOH SC-8020 integrator. An *N*,*N*-dimethylformamide (DMF) solution containing 0.2 M LiBr was used as an eluent at a flow rate of 1 mL/min. Molecular weights of the polymer samples

were calibrated with standard polystyrene samples(TOSOH TSK standard polystyrene).

b. Absorption and Steady-State Fluorescence Spectra. Absorption spectra were recorded on a JASCO V-550 spectrophotometer using a 1 cm path length quartz cuvette. For measurements of absorption spectra of concentrated polymer solutions a flat quartz cell with a 1 mm path length was employed. Steady-state fluorescence spectra were recorded on a Hitachi F-4500 fluorescence spectrometer using a 1 cm path length quartz cuvette. Excitation wavelengths employed were 343 nm for pyrene labels, 337 nm for molecular pyrene probes, and 357 nm for DPH probes. The width of both excitation and emission slits was maintained at 2.5 and 5.0 nm for pyrene and DPH fluorescence measurements, respectively. All spectra were measured with air-equilibrated polymer solutions at room temperature.

Aqueous solutions of molecular pyrene of known concentrations were prepared by diluting a pyrene-saturated aqueous solution prepared as reported previously.[14] Sample solutions for spectroscopic measurements were prepared by dissolving a known amount of polymer in an aqueous pyrene solution of a known concentration.

An aqueous solution of DPH was prepared by injecting a small amount of a tetrahydrofuran (THF) solution of DPH into pure water. The concentration of DPH was adjusted to 9.6×10^{-7} M. The aqueous solution of DPH thus prepared contained 0.04% (w/w) THF. Sample solutions for fluorescence measurements were prepared by dissolving dry polymer samples in the DPH aqueous solution. The final concentrations of the polymer and DPH were adjusted to 0.2 g/dL and 9.6×10^{-7} M, respectively.

c. Fluorescence Decays. Fluorescence decays were measured by a time-correlated single-photon counting technique using a Horiba NAES 550 system equipped with a flash lamp filled with H_2. This system allows us to measure decay and response functions simultaneously. Pyrene labels were excited at 343 nm, and fluorescence was monitored at a wavelength in the neighborhood of 400 nm through combined band-pass (Toshiba KL-40) and cutoff (Toshiba L-38) filters. The decay data were analyzed by a conventional deconvolution technique.

d. Nonradiative Energy Transfer (NRET). Sample solutions of the doubly labeled polymers with varying f_{Dod} (polymer concentration is 5×10^{-3} g/dL) were excited at 290 nm, and steady-state fluorescence spectra were recorded. The ratio of the intensities of pyrene fluorescence to naphthalene fluorescence (I_{Py}/I_{Np}), which is a measure for an NRET efficiency, was calculated from the fluorescence intensities around 337 and 376 nm for naphthalene and pyrene fluorescence, respectively. Although naphthalene can be almost selectively excited at 290 nm, there is a small contribution of direct excitation of pyrene at this wavelength. This contribution was corrected by subtracting the fluorescence spectrum of the corresponding pyrene singly labeled polymer of the same pyrene concentration from each spectrum observed for the doubly labeled polymers.[7]

e. Quasielastic Light Scattering (QELS). QELS data were obtained at varying scattering angles ($\theta = 50°$, 70°, 90°, 110°, and 130°) at 25 °C with an Otsuka Electronics Photal DLS-7000 light scattering spectrometer equipped with an Ar laser (60 mW at $\lambda = 488$ nm) and an ALV-5000 multi-τ digital time correlator. Sample solutions were filtered with a 0.2 μm membrane filter prior to measurement.

The intensity autocorrelation function, $g^{(2)}(t)$, is related to the normalized autocorrelation function, $g^{(1)}(t)$, as

$$g^{(2)}(t) = B[1 + \beta|g^{(1)}(t)|^2] \tag{1}$$

where β is a constant parameter of the optical system and B is a baseline term. To obtain relaxation time distribution, the inverse Laplace transform (ILT) analysis for the intensity autocorrelation function was performed by conforming the REPES algorithm[15] as follows:

$$g^{(1)}(t) = \int \tau A(\tau) \exp(-t/\tau)\, \mathrm{d} \ln \tau \tag{2}$$

The relaxation time distributions are presented as a $\tau A(\tau)$ vs $\log \tau$ profile. Diffusion coefficients, D, are calculated from the average relaxation rates (Γ) as

$$D = (\Gamma/q^2)_{q \to 0} \tag{3}$$

where q is the magnitude of scattering vector expressed as $q = (4\pi n/\lambda) \sin(\theta/2)$ where n is the index of refraction of the solution. The hydrodynamic radius R_h was calculated using the Einstein−Stokes equation

$$R_h = k_B T/6\pi\eta D \tag{4}$$

where k_B is Boltzmann's constant, T is the absolute temperature, and η is the solvent viscosity.

f. Determination of Aggregation Number (N_{agg}). The numbers of polymer-bound dodecyl groups aggregated in a hydrophobic domain were determined by a time-resolved fluorescence technique using pyrene as a probe. Pyrene was solubilized in hydrophobic microdomains formed by the polymers at a pyrene concentration high enough for excimer to be formed within the hydrophobic microdomain. Sample solutions were filtered with a 0.2 μm membrane filter prior to measurement. Fluorescence decays for pyrene probes solubilized in polymer solutions were observed using combined band-pass and cutoff filters (Toshiba KL-40 and L-38, respectively). Monomeric pyrene fluorescence decay data were fitted to a kinetic model developed by Infelta[16] and Tachiya[17]in the form of

$$\ln[I(t)/I(0)] = A_3[\exp(-A_4\, t) - 1] - A_2 t$$

$$A_2 = k_0 + n_Q k_Q k^-/(k_Q + k^-)$$

$$A_3 = n_Q k_Q{}^2/(k_Q + k^-)^2$$

$$A_4 = k_Q + k^- \tag{5}$$

where $I(t)$ and $I(0)$ are the fluorescence intensities at time t and 0 following light pulse excitation, respectively, k_Q is the pseudo-first-order rate constant for quenching of excited pyrene, k_0 ($=\tau_0^{-1}$) is the fluorescence decay rate constant for pyrene inside the micelle without excimer formation, n_Q is the average number of quenchers dissolved in a micelle, and k^- is the first-order rate constant for exit of a pyrene molecule from a micelle. n_Q can be expressed as $[Q]_m/[M]$, where $[Q]_m$ is the molar concentration of quencher inside micelle and [M] is the molar concentration of micelles. Because the quenching of monomeric pyrene fluorescence is due to the excimer formation of pyrene, $[Q]_m$ corresponds to the concentration of pyrene. The $[Q]_m/[M]$ ratio was determined from the best fit, and values of N_{agg} were calculated from the $[Q]_m/[M]$ ratios.

Results and Discussion

Characterization of the Polymers. The degrees of hydrophobic modification (i.e., f_{Dod}) for the polymers employed in the present work are listed in Table 1 along with their molecular weight data. The content of pyrene labels in Py-DDA-PASP and Np-Py-DDA-PASP with varying f_{Dod} is 1 mol % while the content of naphthalene labels in all the Np-Py-DDA-PASP samples is 4 mol %. The number- and weight-average molecular weights, M_n and M_w, respectively, and molecular weight distributions (M_w/M_n) presented in Table 1 are those measured with polymers in the hydrophobically modified PSI form (i.e., before SI units are converted into ASP units by hydrolysis). Since the polymers before hydrolysis are soluble in DMF, we performed GPC measurements using a 20 mM LiBr DMF solution as an eluent. Molecular weights were calibrated with polystyrene standards. As we employed the same PSI as the starting material for the reaction with dodecylamine, M_n of DDA-

Table 1. Contents of Dodecyl Moieties in the Polymers and Their Molecular Weights

f_{Dod}[a] (mol %)	M_w[b] ($\times 10^4$)	M_n[b] ($\times 10^4$)	M_w/M_n[b]	$M_{n,calc}$[c] ($\times 10^4$)
		DDA-PASP		
0	1.7	1.3	1.3	
3	1.5	1.0	1.5	1.4
14	2.1	1.5	1.4	1.6
22	1.8	1.2	1.5	1.8
31	1.9	1.3	1.5	2.1
48	2.0	1.3	1.5	2.5
		Py-DDA-PASP		
0	1.7	1.3	1.3	
4	1.8	1.2	1.5	1.4
14	2.1	1.5	1.4	1.7
22	1.9	1.2	1.5	1.9
32	1.9	1.3	1.5	2.1
47	2.1	1.4	1.5	2.5
		Np-Py-DDA-PASP		
0	1.8	1.3	1.4	
5	2.0	1.6	1.2	1.5
12	2.2	1.7	1.3	1.7
21	2.2	1.7	1.3	1.9
31	2.1	1.6	1.3	2.2
43	2.1	1.6	1.3	2.5

[a] Determined by ^{1}H NMR spectra. [b] Determined by GPC in a 20 mM LiBr DMF solution calibrated with polystyrene standards for the polymers before SI units are converted into ASP units by hydrolysis. [c] Calculated M_n for DDA-PASP (both nonlabeled and labeled) on the basis of f_{Dod} and M_n of PSI.

PASP can be calculated using M_n of PSI and f_{Dod} of the product. These calculated M_n values for DDA-PASP, Py-DDA-PASP, and Np-Py-DDA-PASP are given in Table 1. For the calculation of M_n of the labeled polymers, the contents of pyrene and naphthalene labels were taken into account. The calculated M_n values for all the polymers are more or less the same, ranging from 1.4 to 2.5 $\times 10^4$. All the polymers are soluble in water at pH $\geq$ 7, but the polymers with $f_{Dod} \geq 43$ mol % are only slightly soluble in water at pH = 4.

Steady-State and Time-Dependent Fluorescence of Pyrene-Labeled Polymers. Steady-state fluorescence spectra of pyrene provide information about microenvironmental polarity. The intensity ratio of the third to the first vibronic peaks (I_3/I_1) is sensitive to the polarity of media where pyrene exists, the I_3/I_1 ratio showing a larger value in less polar media.[18]

Steady-state fluorescence spectra of pyrene molecules solubilized in DDA-PASP (nonlabeled polymers) in aqueous solutions show an increase in the I_3/I_1 ratio as f_{Dod} is increased. The I_3/I_1 ratios are plotted in Figure 1 as a function of f_{Dod} for DDA-PASP in aqueous solutions at pH = 9 without added salt. Aqueous solutions employed for these fluorescence measurements contained 7 $\times 10^{-7}$ M pyrene (a saturated concentration of pyrene in pure water[19]) and 5 $\times 10^{-2}$ g/dL DDA-PASP.

The relationship between the I_3/I_1 ratio and f_{Dod} for Py-DDA-PASP in aqueous solutions at pH = 9 without added salt, reported in an earlier paper,[4] is also presented in Figure 1 for comparison. The pyrene labels in Py-DDA-PASP show an increase in the I_3/I_1 ratio with increasing f_{Dod}, but the I_3/I_1 values at all f_{Dod} are significantly smaller than those observed for molecular pyrene probes solubilized in the nonlabeled polymers of the same f_{Dod}. With the pyrene label, as compared to molecular pyrene probes solubilized, a relatively large increase in the I_3/I_1 ratio was observed at f_{Dod} < ca. 5 mol %, and the increase becomes more gradual at f_{Dod} > ca. 5 mol % as f_{Dod} is increased. This observation suggests that hydrophobic association of polymer-bound

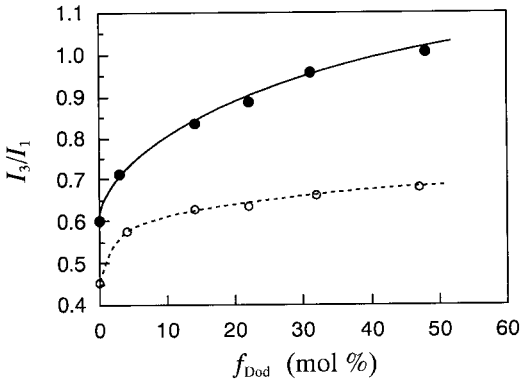

Figure 1. I_3/I_1 ratios in pyrene fluorescence spectra of molecular pyrene probes ([pyrene] = 7 $\times 10^{-7}$ M) solubilized in aqueous solutions of 0.05 g/dL DDA-PASP (●) and of pyrene labels in Py-DDA-PASP (○)[4] plotted as a function of f_{Dod} at pH = 9 without added salt.

dodecyl groups starts to occur at a relatively low f_{Dod} (<5 mol %), and pyrene labels are incorporated in hydrophobic microdomains formed. The extent of the label incorporation into hydrophobic microdomains increases as f_{Dod} is increased.

In our previous work on different types of hydrophobically modified polyelectrolytes labeled with the same type of pyrene labels (e.g., the terpolymers of AMPS, DodMAm, and a small mole fraction of *N*-(1-pyrenylmethyl)methacrylamide), we confirmed that the I_3/I_1 values indicated by pyrene labels were virtually the same as those indicated by molecular pyrene probes solubilized in the corresponding nonlabeled copolymers of the same hydrophobe contents.[7] This indicates that the observed smaller I_3/I_1 values for Py-DDA-PASP are not due to the nature of the pyrene labels employed (i.e., pyrene substituted with a carbonylaminomethyl group at the 1-position). A structural feature for DDA-PASP is that there are a large number of amide bonds in the polymer backbone and side chain (Chart 1). Since pyrene labels are covalently confined closely to the polymer backbone, the labels may experience microenvironments that are crowded with dipoles of the amide bonds. Such microenvironments may be responsible for the observed smaller I_3/I_1 values indicated by the pyrene labels in Py-DDA-PASP. On the other hand, molecular pyrene probes may be solubilized in the core of hydrophobic microdomains such that the probes can experience hydrophobic microenvironments where the effect of the polymer backbone is shielded.

It is known that the fluorescence lifetime of pyrene is longer in hydrophobic media than in hydrophilic media.[20] Fluorescence decay data obtained for Py-DDA-PASP in aqueous solutions at pH = 9 without added salt are presented in Table 2. Decay data for f_{Dod} = 0 mol % (i.e., Py-labeled PASP without hydrophobes) were best-fitted to a single-exponential function whereas the data for $f_{Dod} \geq 3$ mol % were best-fitted to a double-exponential function with χ^2 ranging 1.00−1.25. The lifetimes for the fast decay component, ranging 142−170 ns, may correspond to pyrene labels exposed to the water phase, whereas those for the slow decay component, ranging 340−359 ns, may correspond to the labels incorporated in hydrophobic microdomains. The fractions of the short and long lifetime components are plotted as a function of f_{Dod} in Figure 2a. A large increase in the fraction of the long lifetime component and, in turn, a large decrease in the fraction of the short

Table 2. Fitting Parameters for Fluorescence Decays for Pyrene Labels in Py-DDA-PASP with Varying f_{Dod} Measured in 0.05 M NaCl at pH = 9[a]

f_{Dod} (mol %)	τ (ns)/α	$\langle\tau\rangle^b$ (ns)	χ^2
0	178/1.0	178	1.16
3	170/0.648, 341/0.352	230	1.25
14	142/0.470, 341/0.530	247	1.24
22	144/0.458, 340/0.542	250	1.22
32	151/0.420, 353/0.580	268	1.00
47	164/0.309, 359/0.691	299	1.17

[a] Fitting function; $I(t) = \sum\alpha_i \exp(-t/\tau_i)$, where τ_i is the fluorescence lifetime of the ith component and a_i is its fraction. [b] Average lifetime calculated using $\langle\tau\rangle = \sum(\alpha_i\tau_i/\alpha_i)$.

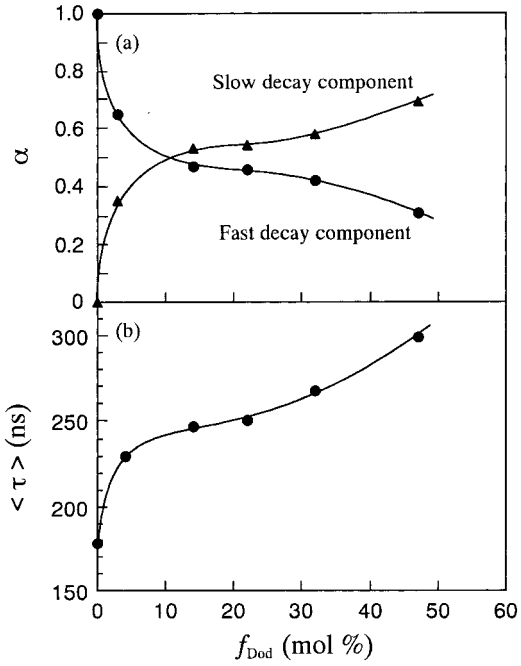

Figure 2. Fractions of the short and long lifetime components (a) and the averaged fluorescence lifetime (b) for Py-DDA-PASP plotted as a function of f_{Dod} at pH = 9 without added salt.

lifetime component upon increase in f_{Dod} were observed at f_{Dod} < ca. 15 mol %. At higher f_{Dod}, the changes in the fractions of the long and short lifetime components become gradual. This tendency is similar to that observed with the I_3/I_1 ratio for Py-DDA-PASP (Figure 1). These observations indicate that a significant extent of hydrophobic associations of PASP-bound dodecyl groups occurs at f_{Dod} < ca. 15 mol %. A significant fraction of pyrene labels are incorporated in hydrophobic domains at f_{Dod} < ca. 15 mol %, and the fraction increases rather gradually as f_{Dod} is increased at f_{Dod} > ca. 15 mol %. The average lifetime increases with an increase in f_{Dod} significantly in the region 0 < f_{Dod} < 3 mol % (Figure 2b). This tendency is similar to the tendency observed for the slow decay component shown in Figure 2a.

As the fluorescence quantum yield of DPH depends strongly on the solvent polarity, DPH can be used as a sensitive probe to monitor the formation of hydrophobic domains. The fluorescence intensity of DPH is very strong in hydrophobic media whereas it fluoresces only weakly in hydrophilic media.[21] In Figure 3a, the fluorescence intensity of DPH in aqueous solutions of DDA-PASP at varying pH without added salt is plotted against f_{Dod}. The fluorescence intensity increases gradually with increasing f_{Dod} up to ca. 20 mol % and then increases more significantly at higher f_{Dod}. This result

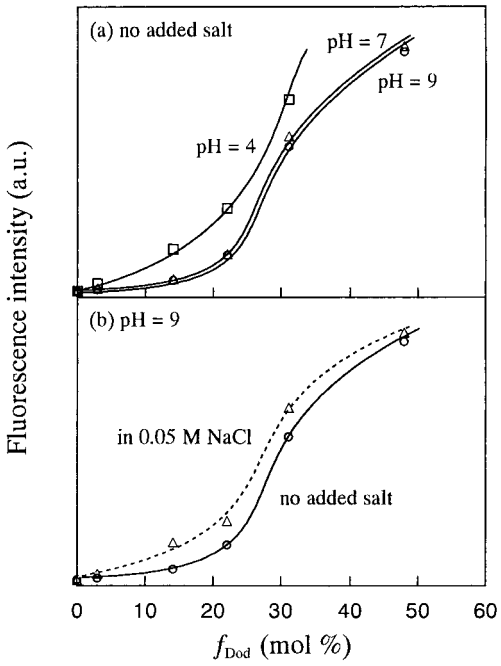

Figure 3. Intensities of fluorescence emitted from DPH probes plotted as a function of f_{Dod} for DDA-PASP at pH = 4, 7, and 9 without added salt (a) and at pH = 9 with and without 0.05 M NaCl (b). [Polymer] = 0.2 g/dL; [DPH] = 9.6×10^{-7} M; Excitation at 357 nm.

indicates that DPH probes are solubilized in the microdomains rather gradually with increasing f_{Dod} at f_{Dod} < ca. 20 mol %, but the probes are more significantly solubilized at higher f_{Dod}. At pH = 4, the fluorescence intensity is higher than those at pH = 7 and 9 at all f_{Dod}, indicating that the hydrophobic association is enhanced at lower pH because of decreased electrostatic repulsions in polymer chains. Figure 3b compares the plots of the fluorescence intensity against f_{Dod} at pH = 9 with and without added salt ([NaCl] = 0.05 M). The added salt induces the formation of hydrophobic domains at lower f_{Dod} due to the shielding of electrostatic repulsions.

The profiles of the fluorescence intensity for DPH probes as a function of f_{Dod} are quite different from the profiles of the I_3/I_1 ratio (Figures 1) and of fluorescence lifetime (Figure 2) for Py-DDA-PASP. These observations are not well-understood at the moment, but a plausible explanation is that a larger hydrophobic microdomain in size may be necessary for the solubilization of DPH in hydrophobic domains than the solubilization of pyrene, and hence a significant change in the fluorescence intensity for DPH occurs when hydrophobic microdomains grow large enough to accommodate DPH at a larger f_{Dod} than in the pyrene case.

NRET in Doubly-Labeled Polymers. Naphthalene and pyrene are often employed as an energy donor/acceptor pair for NRET studies[22−26] due to the fact that the naphthalene emission and pyrene absorption have a large spectral overlap and that naphthalene can be selectively excited at 290 nm. NRET occurs when naphthalene and pyrene come close to each other within the Förster radius (R_0 = 2.86 nm for transfer from 1-methylnaphthalene to pyrene[27]). Changes in the extent of NRET can be represented by the intensity ratio of pyrene fluorescence to naphthalene fluorescence (I_{Py}/I_{Np}), an increase in the I_{Py}/I_{Np} ratio indicating a decrease in the average distance between naphthalene and

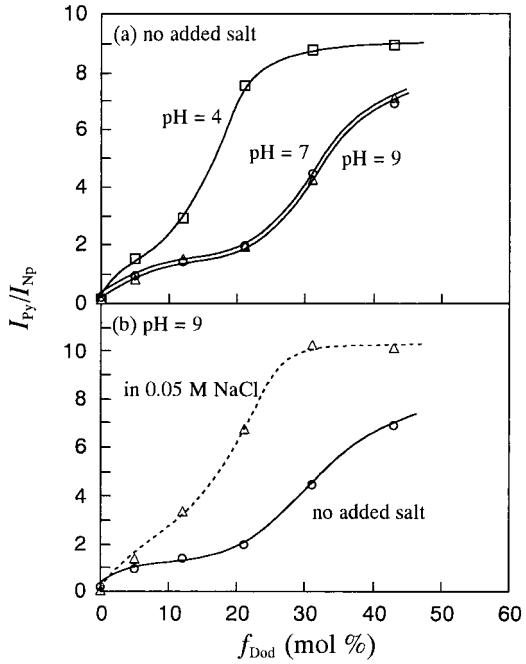

Figure 4. Ratios of the intensities of fluorescence from pyrene and naphthalene labels (I_{Py}/I_{Np}) plotted as a function of f_{Dod} for Np-Py-DDA-PASP at pH = 4, 7, and 9 without added salt (a) and at pH = 9 with and without 0.05 M NaCl (b). [Polymer] = 5×10^{-3} g/dL. Excitation at 290 nm.

pyrene. Thus, intrapolymer NRET in polymers labeled doubly with pyrene and naphthalene is expected to provide information about conformational dimension of the polymer in solution.

In Figure 4a, I_{Py}/I_{Np} ratios are plotted as a function of f_{Dod} for Np-Py-DDA-PASP in aqueous solutions at pH = 4, 7, and 9 without added salt. At pH = 7 and 9, the I_{Py}/I_{Np} ratio increases gradually with increasing f_{Dod} up to ca. 20 mol %, but the ratio increases more significantly at $f_{Dod} > 20$ mol %. This indicates that a significant decrease in the average distance between the naphthalene and pyrene labels in the polymer starts to occur at f_{Dod} near 20 mol %. This chain compaction proceeds significantly in a region $20 < f_{Dod} < 40$ mol % due to extensive intrapolymer hydrophobic associations of dodecyl groups. At lower pH, the f_{Dod} range where the I_{Py}/I_{Np} ratio significantly increases shifts toward smaller f_{Dod}; e.g., at pH = 4, the I_{Py}/I_{Np} ratio increases significantly in the range $5 < f_{Dod} < 20$ mol %, reaching a plateau at f_{Dod} near 30 mol %. This indicates that with decreasing pH hydrophobic associations occur at lower f_{Dod} because of a decreased electrostatic repulsion in the polymer at lower pH. This electrostatic effect was manifested by an effect of added salt. Figure 4b compares plots of the I_{Py}/I_{Np} ratio against f_{Dod} at pH = 9 in aqueous solutions with and without added salt. In the presence of 0.05 M NaCl, a large increase in the I_{Py}/I_{Np} ratio is observed at lower f_{Dod}, showing a saturation tendency near $f_{Dod} = 30$ mol %. This indicates that polymer-bound dodecyl groups can associate more easily in the presence of salt than in pure water due to an electrostatic shielding effect.

The profiles of the I_{Py}/I_{Np} ratio as a function of f_{Dod} are quite different from those of the I_3/I_1 ratio (Figure 1) and fluorescence lifetime (Figures 2) but rather similar to those of the fluorescence intensity for DPH probes at pH = 7 and 9 (Figure 3). The I_{Py}/I_{Np} ratio should undergo a particularly large change in response

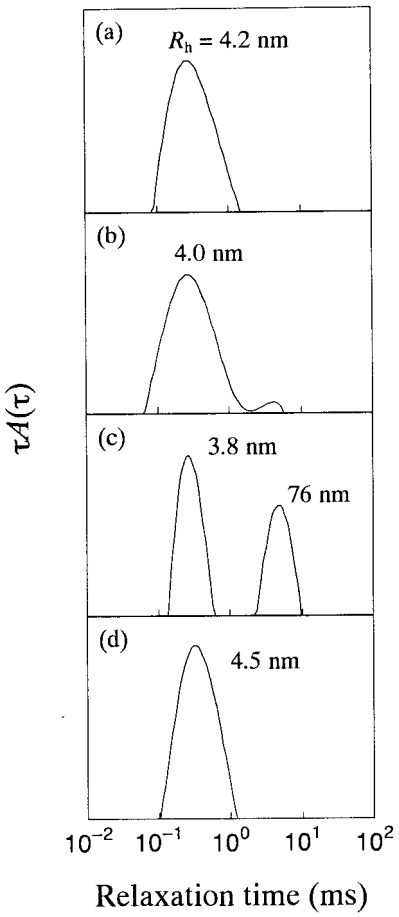

Figure 5. Distributions of relaxation times in QELS at θ = 90° for DDA-PASP with f_{Dod} = 14 (a), 22 (b), 31 (c), and 48 mol % (d) at 0.25 g/dL polymer in 0.05 M NaCl aqueous solutions at pH = 9.

to a change in the conformational dimension on a length scale of R_0 whereas the I_3/I_1 ratio and the fluorescence lifetime would change in accordance with a change in the micropolarity in the immediate vicinity of pyrene labels. In the case of the pyrene-labeled polymer with f_{Dod} = 14 mol % in aqueous solutions at pH = 9 without added salt, it is suggested from the fluorescence decay results listed in Table 2 that more than a half of pyrene labels are incorporated in hydrophobic microdomains, and relatively large increases in the I_3/I_1 ratio and in the average lifetime are observed in the region $0 < f_{Dod} < 15$ mol %, these increases being much more gradual in the region $15 < f_{Dod} < 50$ mol %. In contrast, the increase in the I_{Py}/I_{Np} ratio with increasing f_{Dod} at pH = 9 without added salt is only gradual in the region $0 < f_{Dod} < 20$ mol %, but a pronounced increase occurs in the region $20 < f_{Dod} < 50$ mol %. Therefore, it can be concluded that a considerable decrease in the conformational dimension (i.e., collapse) of the polymer chain with respect to a length scale of R_0 takes place after a large portion of pyrene labels are incorporated in hydrophobic microdomains formed by polymer-bound dodecyl groups. In contrast, the solubilization of DPH probes is suggested to occur significantly when the polymer chain collapses into a compact conformation.

QELS of Nonlabeled Polymers. Figure 5 shows QELS relaxation time distributions for DDA-PASP with varying f_{Dod} observed at 0.25 g/dL polymer in 0.05 M NaCl aqueous solutions of pH = 9. The plot of the relaxation rate (Γ) (i.e., the reciprocal of the relaxation

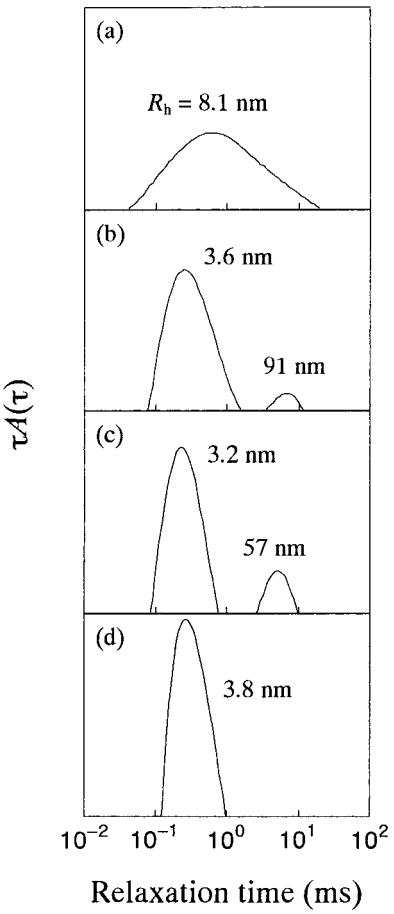

Figure 6. Distributions of relaxation times in QELS at θ = 90° for DDA-PASP with f_{Dod} = 3 (a), 14 (b), 22 (c), and 48 mol % (d) at 1.0 g/dL polymer in 0.05 M NaCl aqueous solutions at pH = 9.

time) at each distribution peak top as a function of the square of the scattering vector (q^2) yielded a straight line passing through the origin (data not shown). Thus, all the relaxations observed are due to a diffusive mode. An apparent hydrodynamic radius (R_h) for each peak calculated from the diffusion coefficient (D) estimated from the slope of the $\Gamma - q^2$ plot (see Experimental Section) is indicated in Figure 5. QELS data for DDA-PASP with f_{Dod} = 0 and 3 mol % are not included in Figure 5 because scattering intensities of these polymers at the concentration of 0.25 g/dL were too weak to be able to perform accurate analysis. The relaxation time distribution for the polymer with f_{Dod} = 14 mol % is apparently unimodal at this polymer concentration with an R_h of 4.2 nm, suggesting that the polymer exists as a unimer state (single molecular state) or as an aggregate consisting of a small number of polymer chains. Therefore, the formation of hydrophobic domains that are indicated by pyrene fluorescence data at f_{Dod} < 15 mol % (Figures 1 and 2) may be due to dominantly intrapolymer hydrophobic associations. As the polymer concentration is increased to 1.0 g/dL, the relaxation time distribution for the polymer with f_{Dod} = 14 mol % becomes bimodal with another peak appearing at a longer relaxation time (Figure 6). Thus, this polymer shows a tendency to undergo interpolymer associations with increase in the polymer concentration. Such a tendency is more significant for the polymers with higher f_{Dod}. In the case of f_{Dod} = 22 mol %, a small peak with a longer relaxation time already exists at a polymer concentration of 0.25 g/dL. The intensity of the slow mode peak, relative to the fast mode peak, increases with increasing polymer concentration (Figure 6). The occurrence of the slow relaxation mode becomes more significant as f_{Dod} is increased to 31 mol %. The relaxation time distributions are clearly bimodal with fast and slow mode relaxation peaks even at 0.25 g/dL polymer (Figure 5). Values of R_h for the relaxation times at the peak top of the fast and slow mode distributions for f_{Dod} = 31 mol % are 3.8 and 76 nm at 0.25 g/dL polymer, respectively. As the polymer concentration was increased to 1.0 g/dL, the polymer with f_{Dod} = 31 mol % was not completely soluble in 0.05 M NaCl but gel-like particles were found in solutions. Therefore, we were unable to perform QELS measurements with a 1.0 g/dL solution of this polymer. As f_{Dod} is further increased to 48 mol %, the QELS relaxation time distributions are unimodal regardless of the polymer concentration. The profile of the relaxation time distribution, and the relaxation time at the peak top as well, remains almost the same over the range of the polymer concentrations studied (0.25−1.0 g/dL). This observation suggests that the polymer with f_{Dod} = 48 mol % yields a compact association structure independent of the polymer concentration.

Aggregation Number of Hydrophobes. Since DDA-PASP with f_{Dod} = 48 mol % forms a single association species with a compact structure over a significant range of polymer concentrations, we attempted to estimate the mean aggregation number of dodecyl groups (N_{agg}) in the association structure using a time-resolved fluorescence method. Pyrene probes were solubilized in hydrophobic domains of the polymer in aqueous solutions. If a hydrophobic domain contains two or more pyrene probes, excimer may be formed within the domain. In such a case, monomeric pyrene fluorescence should be quenched via the excimer formation, and hence a shorter lifetime component due to the quenching may be observed in fluorescence decay profiles. Such fluorescence decay data can be fitted to a kinetic equation proposed by Infelta[16] and Tachiya[17] (eq 5), allowing us to calculate n_Q, the molar concentration of pyrene inside the hydrophobic domain relative to the molar concentration of the hydrophobic domain, from eq 6.

$$n_Q = (A_3A_4 + A_2 - k_0)^2/A_3A_4^2 \qquad (6)$$

From n_Q thus estimated, N_{agg} can be calculated (see Experimental Section).[11] It is important to confirm that there are no other quenching processes involved, but excimer formation and hence a single-exponential fluorescence decay with an unperturbed fluorescence lifetime of pyrene should be observed when the concentrations of pyrene probes solubilized in the hydrophobic domains are sufficiently low. Fluorescence decays for DDA-PASP with f_{Dod} = 48 mol % at a polymer concentration of 0.05 g/dL in 0.05 M NaCl aqueous solutions were carefully examined to verify the applicability of the Infelta−Tachiya kinetics to the present polymer system. In the absence of the polymer, a 0.7 μM pyrene solution in 0.05 M NaCl shows a single-exponential fluorescence decay with a lifetime of 192 ns (χ^2 = 1.21). The concentrations of pyrene were calculated from the absorbance at 338 nm using $\epsilon_{338} = 3.7 \times 10^4$ M^{-1} cm^{-1}.[28] In the presence of DDA-PASP with f_{Dod} = 48 mol %, the decay is single-exponential with a lifetime of 350 ns (χ^2 = 1.03) when the pyrene concentration is lower than ca. 2×10^{-6} M. This indicates that all pyrene molecules

Table 3. Fitting Parameters for the Infelta−Tachiya Equation and Aggregation Numbers of Dodecyl Groups in Hydrophobic Microdomains for DDA-PASP with f_{Dod} = 48 mol % Measured in 0.05 M NaCl at pH = 9

[polymer] (g dL^{-1})	[pyrene][a] (10^{-4} M)	A_4 (10^{-6} s^{-1})	A_3	A_2 (10^{-6} s^{-1})	k_0 (10^{-6} s^{-1})	χ^2	N_{agg}
0.05	0.276	2.49	1.76	2.51	2.86	0.85	62
0.10	0.524	2.47	1.69	2.69	2.72	0.89	73
0.25	1.274	3.31	1.37	2.92	2.77	0.88	67
0.75	4.000	3.11	1.56	2.69	2.78	1.05	65
1.00	5.153	3.17	1.59	2.74	2.66	1.09	73
							av 68

[a] Concentrations were calculated from the absorbance at 338 nm using $\epsilon_{338} = 3.7 \times 10^4$ M^{-1} cm^{-1}.[28]

are solubilized in hydrophobic domains formed by polymer-bound dodecyl groups, and no pyrene remains in the bulk water phase. The decay data for the polymer with f_{Dod} = 48 mol % (0.05 g/dL) observed at a higher concentration of pyrene are best-fitted to eq 5 with χ^2 = 0.85 (Table 3). From the best fit, all the parameters in eq 5 can be determined, thus allowing us to calculate N_{agg} to be 62. We performed fluorescence decay measurements with several different polymer concentrations and the pyrene concentrations. Fitting parameters and N_{agg} values obtained are listed in Table 3. At all the concentrations of the polymer and pyrene investigated, N_{agg} values obtained lie in a range of 62−73 without any particular tendency to depend on the polymer and pyrene concentrations. Therefore, all the N_{agg} values are averaged to obtain a value of 68 (Table 3).

The degree of polymerization of PSI employed for the synthesis of DDA-PASP is calculated from M_n (Table 1) to be ca. 130. Therefore, in the case of DDA-PASP with f_{Dod} = 48 mol %, the number of dodecyl groups per polymer chain can be calculated to be ca. 62. This number is quite close to the average N_{agg} value of 68 listed in Table 3. This suggests that the compact association species formed from DDA-PASP with f_{Dod} = 48 mol % is a unimolecular micelle resulting from completely intramolecular hydrophobe associations. However, we cannot totally rule out a possibility that the association structure is comprised of two or more polymer chains, consisting of two or more hydrophobic domains of an N_{agg} of ca. 68. However, it may be reasonable to conceive that this possibility is very small, given the small hydrodynamic size of the association structure that is independent of the polymer concentration (Figures 5 and 6).

Conclusions

The self-association behavior of hydrophobically modified PASP, synthesized by treating PSI with dodecylamine followed by hydrolysis, was characterized by fluorescence and QELS techniques as a function of the content of dodecyl groups in the polymer. For fluorescence studies, the polymers were labeled singly with pyrene, Py-DDA-PASP, and doubly with naphthalene and pyrene, Np−Py-DDA-PASP. The I_3/I_1 ratios for Py-DDA-PASP and for molecular pyrene probes solubilized in the polymer phase indicated that the polymer-bound hydrophobes start to associate to form microdomains at a low f_{Dod} near 3 mol %. The pyrene fluorescence lifetime observed for a Py-DDA-PASP solution at pH = 9 also indicated that hydrophobic microdomains were formed at this low f_{Dod}, a significant fraction of pyrene labels being incorporated in the microdomains. Intrapolymer NRET from naphthalene to pyrene labels in Np-Py-DDA-PASP indicated that a considerable decrease in the conformational dimension (i.e., chain compaction) on a length scale of the Förster radius (ca. 2.86 nm) occurred in the region 20 < f_{Dod} < 50 mol % at pH = 9, the region shifting to 10 < f_{Dod} < 30 mol % either upon addition of 0.05 M NaCl at pH = 9 or upon decrease in pH to 4 in the absence of salt. This compaction of the polymer took place after a significant portion of pyrene labels were incorporated in hydrophobic domains formed by polymer-bound dodecyl groups. The collapse of the polymer chain was also able to be monitored by fluorescence of 1,6-diphenyl-1,3,5-hexatriene solubilized in the polymer phase. It was indicated by QELS at pH = 9 in the presence of 0.05 M NaCl that the polymers with $f_{Dod} \leq$ 31 mol % undergo both intra- and interpolymer associations depending on the polymer concentration whereas the polymer with f_{Dod} = 48 mol % shows a strong preference for intrapolymer associations regardless of the polymer concentration. The polymers with $f_{Dod} \leq$ 31 mol % form small aggregates with R_h ranging 3−4 nm and larger aggregates with R_h ranging 60−90 nm coexisting together at pH = 9 in 0.05 M NaCl solutions. The fraction of the larger aggregates increases with polymer concentration. In contrast, the polymer with f_{Dod} = 48 mol % forms only small aggregates with R_h on the order of 4 nm independent of the polymer concentration studied (0.25−1.0 g/dL). The mean aggregation number of dodecyl groups in this small aggregate formed by the polymer with f_{Dod} = 48 mol % was determined to be ca. 68 using a time-resolved fluorescence method. This aggregation number coincides with the number of dodecyl groups per polymer (ca. 62) calculated from the degree of polymerization and f_{Dod} value, suggesting that this small aggregate is a unimolecular micelle. Accordingly, all the smaller aggregates with R_h = 3−4 nm for the polymers with $f_{Dod} \leq$ 31 mol % are also likely to be unimolecular micelles. Thus, DDA-PASP exhibits a strong preference for intrapolymer hydrophobe associations to form a unimolecular micelle if the hydrophobe content is as high as 48 mol %.

Acknowledgment. This work was supported in part by a Grant-in-Aid for Scientific Research No. 10450354 from the Ministry of Education, Science, Sports and Culture, Japan, and in part by Shorai Foundation for Science and Technology.

References and Notes

(1) Tomida, M.; Nakato, T.; Kuramochi, M.; Shibata, M.; Matsunami, S.; Kakuchi, T. *Polymer* **1996**, *37*, 4435.
(2) Matsubara, K.; Nakato, T.; Tomida, M. *Macromolecules* **1998**, *31*, 1466.
(3) Tomida, M.; Yabe, M.; Arakawa, Y.; Kunioka, M. *Polymer* **1997**, *38*, 2791.
(4) Nakato, T.; Tomida, M.; Suwa, M.; Morishima, Y.; Kusuno, A.; Kakuchi, T. *Polym. Bull.* **2000**, *44*, 385.
(5) For reviews, see: (a) McCormick, C. L.; Bock, J.; Schulz, D. N. *Encyclopedia of Polymer Science and Engineering*; John Wiley: New York, 1989; Vol. 17, p 730. (b) Bock, J.; Varadaraj, R.; Schulz, D. N.; Maurer, J. J. In *Macromolecular*

Complexes in Chemistry and Biology; Dubin, P., Bock, J., Davies, R. M., Schulz, D. N., Thies, C., Eds.; Springer-Verlag: Berlin, 1994; p 33. (c) Valint, P. L., Jr.; Bock, J.; Schulz, D. N. In *Polymers in Aqueous Media: Performance through Association*; Glass, J. E., Ed.; Advances in Chemistry Series 223; American Chemical Society: Washington, DC, 1989; p 399. (d) *Polymers as Rheology Modifiers*; Schulz, D. N., Glass, J. E., Eds.; Advances in Chemistry Series 462; American Chemical Society: Washington, DC, 1991.

(6) Morishima, Y.; Nomura, S.; Ikeda, T.; Seki, M.; Kamachi, M. *Macromolecules* **1995**, *28*, 2874.
(7) Yamamoto, H.; Mizusaki, M.; Yoda, K.; Morishima, Y. *Macromolecules* **1998**, *31*, 3588.
(8) Yamamoto, H.; Morishima, Y. *Macromolecules* **1999**, *32*, 7469.
(9) Yamamoto, H.; Hashidzume, A.; Morishima, Y. *Macromolecules*, in press.
(10) Yamamoto, H.; Hashidzume, A.; Morishima, Y. *Polym. J.*, in press.
(11) Noda, T.; Morishima, Y. *Macromolecules* **1999**, *32*, 4631.
(12) Chang, Y.; McCormick, C. L. *Macromolecules* **1993**, *26*, 6121.
(13) Hashidzume, A.; Yamamoto, H.; Mizusaki, M.; Morishima, Y. *Polym. J.* **1999**, *31*, 1009.
(14) Yusa, S.; Kamachi, M.; Morishima, Y. *Langmuir* **1998**, *14*, 6059.
(15) Jakes, J. *Czech. J. Phys.* **1988**, *B38*, 1305.
(16) Infelta, P. P.; Grätzel, M.; Thomas, J. K. *J. Phys. Chem.* **1974**, *78*, 190.
(17) Tachiya, M. *Chem. Phys. Lett.* **1975**, *33*, 289.
(18) Kalyanasundaram, K.; Thomas, J. K. *J. Am. Chem. Soc.* **1977**, *99*, 2039.
(19) Yekta, A.; Xu, B.; Duhamel, J.; Adiwidjaja, H.; Winnik, M. A. *Macromolecules* **1995**, *28*, 956.
(20) Morishima, Y.; Tominaga, Y.; Kamachi, M.; Okada, T.; Hirata, Y.; Mataga, N. *J. Phys. Chem.* **1991**, *95*, 6027.
(21) Shinitzky, M.; Barenholz, Y. *J. Biol. Chem.* **1974**, *249*, 2652.
(22) Webber, S. E. *Chem. Rev.* **1990**, *90*, 1469.
(23) Winnik, F. M. *Polymer* **1990**, *31*, 2125.
(24) Ringsdorf, H.; Simon, J.; Winnik, F. M. *Macromolecules* **1992**, *25*, 5353.
(25) Hu, Y.; Kramer, M. C.; Boudreaux, C. J.; McCormick, C. L. *Macromolecules* **1995**, *28*, 7100.
(26) Kramer, M. C.; Steger, J. R.; Hu, Y.; McCormick, C. L. *Macromolecules* **1996**, *29*, 1992.
(27) Berlman, I. B. *Energy Transfer Parameters of Aromatic Compounds*; Academic Press: New York, 1973.
(28) Vorobyova, O.; Yekta, A.; Winnik, M. A. *Macromolecules* **1998**, *31*, 8998.

MA0008342